Available online at www.sciencedirect.com
SCIENCE DIRECT®
European Journal of Mechanics B/Fluids 25 (2006) 18–32

Similarity solutions of energy and momentum boundary layer equations for a power-law shear driven flow over a semi-infinite flat plate

G.E. Cossali

University of Bergamo, Via Marconi 6, 24044 Dalmine, Italy

Received 11 February 2005; accepted 1 April 2005
Available online 9 June 2005

Abstract

The problem of a steady forced convection thermal boundary-layer driven by a power-law shear is investigated. The search for similarity solutions reduces the problem to a couple of ordinary differential equations containing three parameters: the exponent of the decaying exterior velocity profile, the exponent of the power-law prescribing the thermal condition on the wall and Prandtl number. The effects of these parameters on the existence and form of similarity solution are investigated and the functional dependence of the local Nusselt number on these parameters is reported and discussed. An analysis of the assumptions usually accepted to derive similarity solutions is also reported in order to show the range of values of the exterior velocity power-law exponent for which such solutions may exist.

1. Introduction

Convective heat and momentum transfer over a flat plate was the subject of intense studies since the early work of Prandtl [1] in 1904, and the first solutions of the boundary layer momentum and energy equations date back to 1908 [2] and 1921 [3] respectively. Despite such a long history, the problem is still a challenge today, as witnessed by the flourishing of large number of theoretical and numerical studies on this subject in the recent years. As is well known, the convective heat transfer phenomenon depends not only on the form of the imposed thermal boundary conditions on the wall but also on the boundary conditions imposed on the fluid dynamics problem. Then, the classical Blasius problem of a viscous boundary layer over a semi-infinite impermeable flat plate was extended to different wall conditions, such as the case of stretching walls [4–8], and porous media (see for example [9,10]) and it was also shown that a strong analogy exists between this two flows as the ordinary differential problem obtained after the similarity transformation is the same (see for example [13]). The case of the adjustment of the laminar boundary layer to an exterior power-law velocity profile of the form:

$$U = \beta y^{\alpha}, \quad y \to \infty \tag{1}$$

was treated by Weidman et al. [11] for both non-permeable surfaces and free shear layer, and by Magyari et al. [12] for permeable surfaces. Weidman et al. [11] showed that no similarity solution of the momentum equation exists for $\alpha \leqslant -1$, and from the performed numerical experiments they suggested that also for $\alpha \leqslant -2/3$ no solution should exist. They also gave analytical

E-mail address: gianpietro.cossali@unibg.it (G. Cossali).

0997-7546/$ – see front matter
doi:10.1016/j.euromechflu.2005.04.007

Nomenclature

A, B	arbitrary constants
c	specific heat
f	non-dimensional stream function
h	convective heat transfer coefficient
H	enthalpy flux
k	thermal conductivity
L	characteristic length
m	exponent in similarity laws: $m(\alpha)=\frac{\alpha+1}{\alpha+2}$
n	exponent in wall temperature law
P	free stream-wall temperature difference
Pr	Prandtl number
q	heat flux
Q	strength of the heat source
Re	Reynolds number
T	temperature
u	non-dimensional velocity along the plate
$\tilde{u}$	velocity along the plate
U_∞	free stream velocity
v	non-dimensional velocity normal to the plate
$\tilde{v}$	velocity normal to the plate
x	non-dimensional Cartesian coordinate along the plate
$\tilde{x}$	Cartesian coordinate along the plate
y	non-dimensional Cartesian coordinate normal to the plate
$\tilde{y}$	Cartesian coordinate normal to the plate

Greek symbols

α	exponent in free stream velocity profile
β,γ	constants
Δ_2	non-dimensional enthalpy thickness
ζ	non-dimensional variable
η	non-dimensional coordinate
Θ	non-dimensional temperature
ν	kinematic viscosity
ξ	non-dimensional variable
ρ	density
Φ	non-dimensional temperature gradient at the fluid–solid interface
ψ	stream function

Indexes

c	critical
w	wall
∞	free stream

solutions for $\alpha=-1/2$ in terms of Airy functions. Magyari et al. [12] reported, for permeable wall with blowing or suction, that analytical solutions exist for $\alpha=-2/3$ and $\alpha=-1/2$. Under the same boundary conditions (1), Magyari et al. [14] studied the heat transfer characteristics of the boundary layer flow past an impermeable semi-infinite flat plate corresponding to the case $\alpha=-1/2$ and exact analytical solutions were given for the isothermal and the adiabatic wall cases.

One of the objectives of the present paper is to analyse the problem of the forced convection thermal boundary layer under the general case of the power-law velocity profile (that comprises the classical no-shear case) on a semi-infinite flat plate subject to boundary conditions for the energy equation that may assure the existence of similarity solutions, thus extending the study of Weidman et al. [11] to thermally active flows only for the case of bounded flows. This problem has a wide variety of technical and environmental applications, as pointed out in [11] and [14], justifying the interest in finding the conditions for the existence of similarity solutions, which often form the basis of first estimates to the solution of real physical problems. The last section of the paper is devoted to an analysis of the assumptions usually accepted to derive similarity solutions, to show the range of values of the parameter α for which such solutions are expected to exist.

2. Basic equations

Consider an incompressible steady laminar boundary layer flow over a semi-infinite solid flat plate, neglecting buoyancy and viscous dissipation and with zero pressure gradient. Let $\tilde{x}$ and $\tilde{y}$ be the coordinates measured, respectively, along and normal to the plate. Defining the non-dimensional variables:

$$x=\frac{\tilde{x}}{L};\quad y=\frac{\tilde{y}}{L};\quad u=\frac{\tilde{u}L}{\nu};\quad v=\frac{\tilde{v}L}{\nu}$$

the basic equations describing the conservation of mass, momentum and energy in the boundary layer are given by [15]:

$$\frac{\partial u}{\partial x}+\frac{\partial v}{\partial y}=0, \tag{2}$$

$$u\frac{\partial u}{\partial x}+v\frac{\partial u}{\partial y}=\frac{\partial^2 u}{\partial y^2}, \tag{3}$$

$$u\frac{\partial T}{\partial x}+v\frac{\partial T}{\partial y}=\frac{1}{Pr}\frac{\partial^2 T}{\partial y^2}. \tag{4}$$

The mass and momentum equations (2) and (3) must be solved subject to the non-slip boundary conditions on the wall and, following [11] and [14], we will consider the general case of an exterior power law velocity profile:

$$u(x,0)=0; \qquad v(x,0)=0,$$
$$u(x,y\to\infty)=\frac{U_\infty(y)L}{\nu}=\frac{\gamma\tilde{y}^\alpha L}{\nu}=\frac{\gamma y^\alpha L^{1+\alpha}}{\nu}=\beta y^\alpha$$

with $\beta=\gamma L^{1+\alpha}/\nu$. The solution of the steady fluid mechanic problem is classically found by introducing the stream function ψ and by the similarity transformation (see again [11,14]):

$$\eta=yx^{m-1}, \qquad \psi=f(\eta)x^m \tag{5}$$

reducing the momentum equation to the ordinary differential equation:

$$f'''+mff''-f'f'(2m-1)=0 \tag{6}$$

with boundary conditions

$$f'(0)=0; \quad f(0)=0; \quad f'(y=\infty)=\beta\eta^\alpha \tag{7}$$

and the last one imposes $m=\frac{\alpha+1}{\alpha+2}$. It is clear that the parameter α has a basic significance and it is physically more relevant that the similarity parameter m above introduced. For this reason throughout the paper the parameter α will be used to discuss the various cases and $m(\alpha)$ will be employed some time to simplify some equations or some plots.

The characteristic length L can be arbitrarily chosen, in particular the choice:

$$L_1=\left(\frac{\nu}{\gamma}\right)^{1/(1+\alpha)} \quad\Rightarrow\quad \beta=1$$

simplifies the problem and, as pointed out by Weidman et al. [11], the solutions for $\beta\neq 1$ can be obtained by the transformation:

$$L_\beta=\left(\frac{\nu}{\gamma}\right)^{1/(1+\alpha)}\beta^{1/(1+\alpha)}; \qquad \frac{\mathrm{d}^p f_\beta}{\mathrm{d}\eta_\beta^p}=\frac{\mathrm{d}^p f}{\mathrm{d}\eta^p}\beta^{(p+1)/(\alpha+2)}, \tag{8}$$

Due to this degree of freedom, in the remainder of the paper the value of β will be set equal to 1 (and $L=(\nu/\gamma)^{1/(1+\alpha)}$) without loss of generality.

When needed, Eq. (6) was solved numerically by a 4th-order Runge–Kutta method, following a procedure similar to that reported by [11]. The values of $x^{-\alpha/(\alpha+2)}(\mathrm{d}u/\mathrm{d}\eta)_{\eta=0}=f''_\alpha(0)$ were calculated for different values of α and compared (see Fig. 1) to the results reported in [11] with good agreement (to be noticed that the classical no-

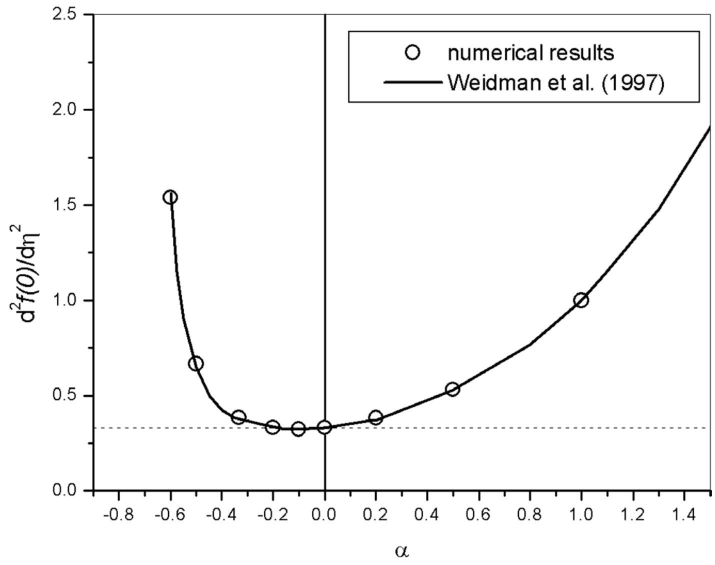

Fig. 1. Values of $f''_\alpha(0)$ for different values of α compared to those found by Weidman et al. [11] (solid line).

shear case gives $f_0''(0) = 0.33206$, and for $\alpha = 1$, the solution is $f_1 = \eta^2/2$ and $f_1''(0) = 1$, i.e. the classical Couette solution).

Considering now the energy equation, under the same assumptions above mentioned it becomes:

$$Pr\, x f_\alpha' T_x - m(\alpha) Pr\, f_\alpha T_\eta - T_{\eta\eta} = 0. \tag{9}$$

In the next sections the conditions for the existence of similarity solutions of Eq. (9) will be discussed.

3. Similarity solutions of the energy equation

Similarity solutions of Eq. (9) can be found by choosing appropriate boundary conditions. Consider the following transformation:

$$T = P(x)\Theta(\eta, x) + T_\infty,$$
$$\Theta(\eta, x) = \frac{T(x,\eta) - T_\infty}{T(x,0) - T_\infty}; \qquad P(x) = T(x,0) - T_\infty$$

it is easy to see that similarity solutions (i.e. Θ explicitly independent of x) of Eq. (9) can be found when $x P_x / P = n = const$, provided $P(x) = T(x,0) - T_\infty \neq 0$, yielding:

$$\Theta_{\eta\eta}^{(n,\alpha)} + m(\alpha) Pr\, f_\alpha \Theta_\eta^{(n,\alpha)} - n Pr\, f_\alpha' \Theta^{(n,\alpha)} = 0, \tag{10}$$
$$\Theta(x,0) = 1; \qquad \Theta(x,\infty) = 0$$

and

$$P(x) = T(x,0) - T_\infty = A x^n. \tag{11}$$

The wall thermal flux is then:

$$q_w = -k \frac{\partial T}{\partial \tilde{y}} = -\frac{k}{L} T_\eta x^{m(\alpha)-1} = \frac{k}{L} A \Phi_{n,\alpha}(Pr) x^{n+m(\alpha)-1} \tag{12}$$

where $\Phi_{n,\alpha}(Pr) = -\Theta_\eta^{(n,\alpha)}(0)$ and the local convective heat transfer coefficient can be written as follows:

$$h = \frac{q_w}{T(x,0) - T_\infty} = \frac{k}{L} \Phi_{n,\alpha}(Pr) x^{m(\alpha)-1}$$

showing that $\Phi_{n,\alpha} x^{(\alpha+1)/(\alpha+2)-1}$ has the physical meaning of a non-dimensional heat transfer coefficient while $\Phi_{n,\alpha}(Pr) x^{(\alpha+1)/(\alpha+2)} = h\tilde{x}/k$ is the local Nusselt number.

To notice (from Eq. (12)) that $\Theta^{(n,\alpha)}$ is also the similarity solution with prescribed wall heat flux distribution given by the power law:

$$q_w = B x^{n+m(\alpha)-1}.$$

The three cases of main practical interest, namely the uniform wall temperature, the uniform wall heat flux and the "adiabatic" wall, are defined by the conditions: $n = 0$, $n = 1 - m(\alpha)$ and $n = -m(\alpha)$ respectively (the last statement stems from Eq. (14)).

Again a 4th-order Runge–Kutta shooting method was used to solve Eq. (10). It is well known that for the classical case of no shear ($\alpha = 0$) the dependence of $\Phi_{n,\alpha}$ on the Prandtl number assumes (for $Pr > 0.6$, see [16,17]) the approximate form: $\Phi_{n,0} = C_{n,0} Pr^{1/3}$ for both the uniform wall temperature ($n = 0$) and uniform heat flux ($n = \frac{1}{2}$) conditions. Figs. 2(a)–2(c) report the values of $C_{n,\alpha} = \Phi_{n,\alpha} Pr^{-1/3}$ for $\alpha = 0$, $\alpha = -1/2$ and $\alpha = 1/2$ and different values of n, showing that the above mentioned dependence still holds for the investigated values of α and n, but the range of validity changes with α: in Figs. 2(a)–(c), the thick solid line indicates where $C_{n,\alpha}$ attains values equal to 0.97 times the asymptotic value. The increase of α increases the range of Pr where the asymptotic approximation holds. It should be noticed that for the classical no-shear case ($\alpha = 0$) with uniform temperature condition ($n = 0$), the value of $C_{0,0}$ is expected to be approximately 0.332 [15] (for $Pr > 0.6$), while with constant heat flux condition ($n = \frac{1}{2}$), $C_{1/2,0}$ is expected to be approximately equal to 0.453 as reported by [15], although in [17] a slightly different value (namely $C_{1/2,0} = 0.460$) was suggested; in the present case a value of $C_{1/2,0} = 0.459$ was found.

Fig. 3(a) shows the value of $\Phi_{n,\alpha}(Pr = 1)$ as a function of n for three different values of α (namely $\alpha = -1/2$, $\alpha = 0$, $\alpha = 1/2$). All the curves pass through the point ($n = -(\alpha+1)/(\alpha+2)$, $\Phi_{n,\alpha} = 0$) and show a similar dependence on n. Fig. 3(b)

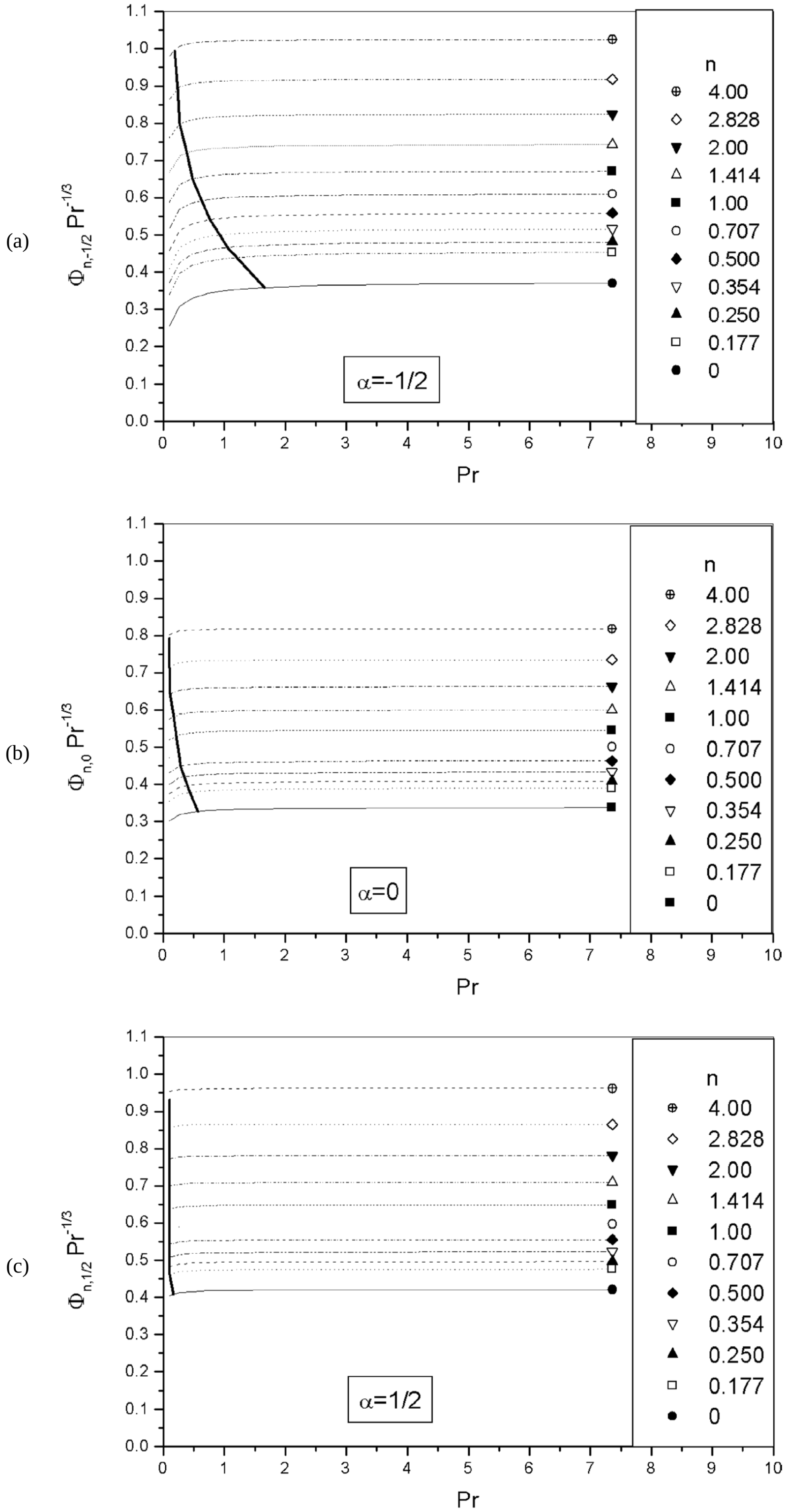

Fig. 2. Values of $C_{n,\alpha} = \Phi_{n,\alpha} Pr^{-1/3}$ as a function of Prandtl number for different values of n and for: (a) $\alpha = -1/2$; (b) $\alpha = 0$; (c) $\alpha = 1/2$.

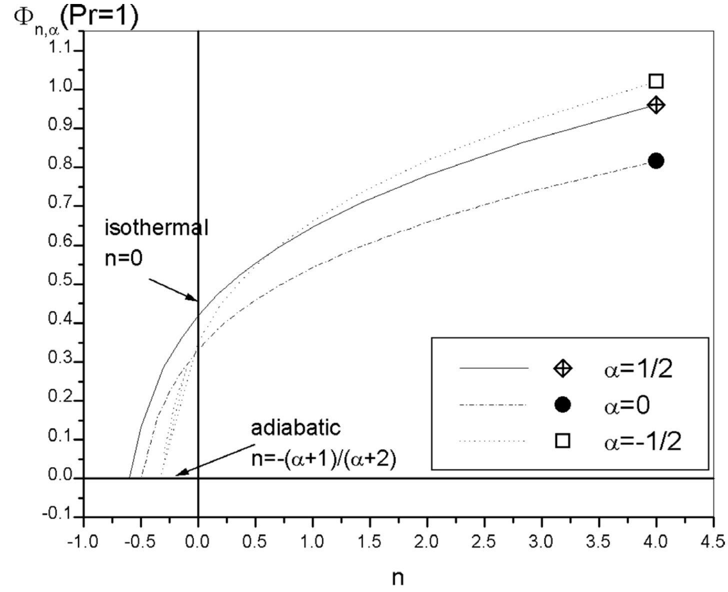

(a)

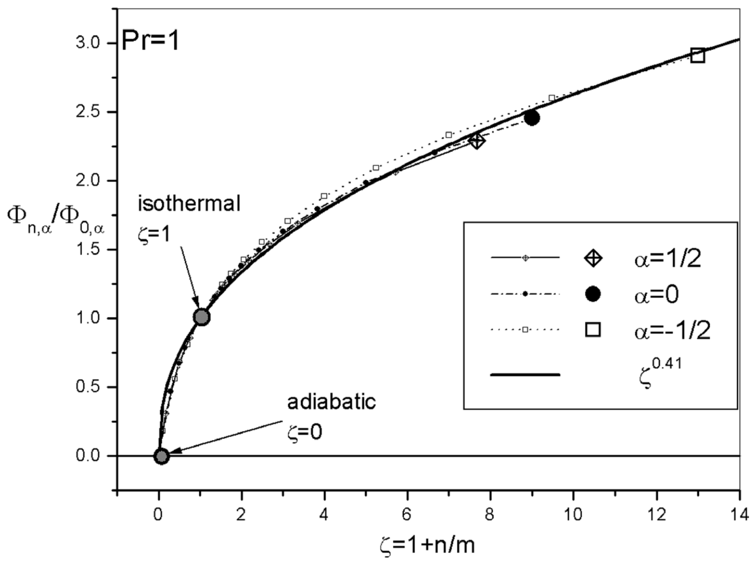

(b)

Fig. 3. (a) Values of $\Phi_{n,\alpha}(Pr=1)$ as a function of n for $\alpha=0,\pm1/2$. (b) Values of $\Phi_{n,\alpha}/\Phi_{0,\alpha}$ for $Pr=1$ as a function of $\zeta=1+n/m(\alpha)$ for $\alpha=0,\pm1/2$.

shows the same curves as a function of: $\zeta=1+n/m(\alpha)$ (where again $m(\alpha)=(\alpha+1)/(\alpha+2)$) and the values of $\Phi_{n,\alpha}/\Phi_{0,\alpha}$ were plotted (for $Pr=1$). The fact that all the curves are close to each other can be understood by the following approximate analysis. On integrating Eq. (10) we obtain after a partial integration and taking into account the boundary conditions:

$$\Phi_{n,\alpha}(Pr)=-m(\alpha)Pr\lim_{\eta\to\infty}f_\alpha\Theta^{(n,\alpha)}+\big(m(\alpha)+n\big)Pr\int_0^\infty f'_\alpha\Theta^{(n,\alpha)}\,\mathrm{d}\eta. \tag{13}$$

Let us conjecture that $\Theta^{(n,\alpha)}$ goes to zero faster than $\eta^{-(\alpha+1)}$ when $\eta\to\infty$ (for $\alpha=-\frac{1}{2}$ this was proven by Magyari et al. [14]), then Eq. (13) becomes:

(a)

(b)

(c)

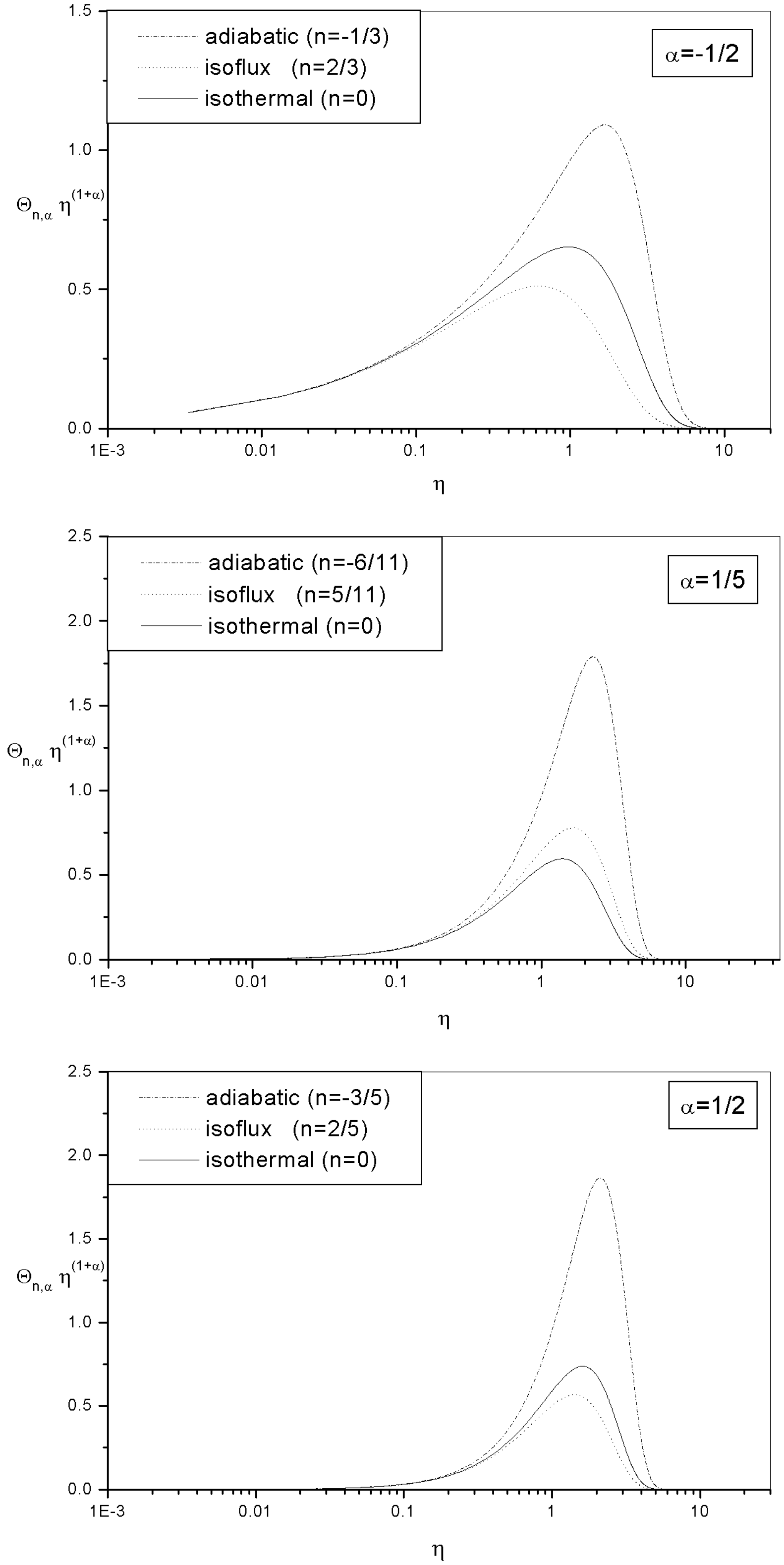

Fig. 4. Plot of the function $\eta^{\alpha+1}\Theta^{(n,\alpha)}$ for different values of α and n.

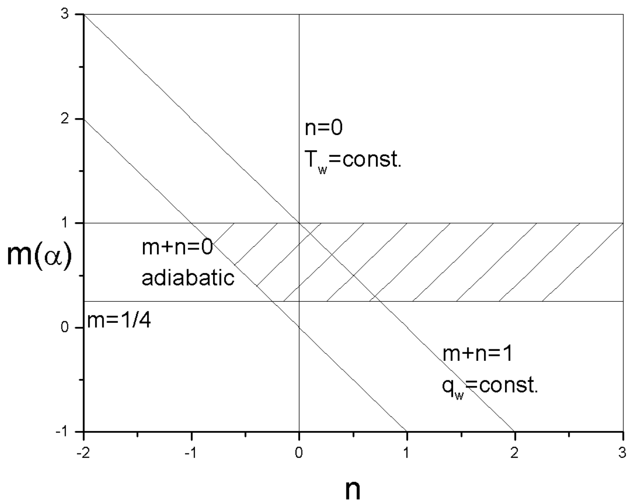

Fig. 5. Region in the (n, m) plane of the expected existence of similarity solutions of the energy boundary layer problem.

$$\Phi_{n,\alpha}(Pr) = \left[m(\alpha) + n\right]Pr \int_0^\infty f'_\alpha \Theta^{(n,\alpha)}\,\mathrm{d}\eta \tag{14}$$

and due to the fact that $0 \leqslant \Theta \leqslant 1$ and $\Phi_{n,\alpha} \geqslant 0$, the condition $n + m(\alpha) \geqslant 0$ must always be fulfilled. Figs. 4 shows the function $\eta^{\alpha+1}\Theta^{(n,\alpha)}$ for some values of (n, α), apparently confirming the validity of the above mentioned conjecture. It should be remembered that, from the analysis reported in [11], similarity solutions of the momentum boundary layer problem (Eqs. (6), (7)) are expected to exist only for $m(\alpha) > 1/4$. Fig. 5 reports instead the region in the (n, m) plane of the expected existence of similarity solutions of the energy boundary layer problem (Eqs. (10)). It should be pointed out that no analysis exists regarding the possible limitations for $n \to \infty$. Consider now the variable $\Phi_{n,\alpha}/\Phi_{0,\alpha}$ plotted in Fig. 3(b), from Eq. (14):

$$\frac{\Phi_{n,\alpha}}{\Phi_{0,\alpha}} = \frac{(m(\alpha) + n)Pr\int_0^\infty f'_\alpha \Theta^{(n,\alpha)}\,\mathrm{d}\eta}{m(\alpha)Pr\int_0^\infty f'_\alpha \Theta^{(0,\alpha)}\,\mathrm{d}\eta} = \zeta\frac{\int_0^\infty f'_\alpha \Theta^{(n,\alpha)}\,\mathrm{d}\eta}{\int_0^\infty f'_\alpha \Theta^{(0,\alpha)}\,\mathrm{d}\eta}$$

from the shape of the variables $\Theta^{(n,\alpha)}$ and f'_α a rough approximation of the integrands is given by:

$$\Theta^{(n,\alpha)} = \begin{cases} 1 - \Phi_{n,\alpha}\eta & \text{for } \xi = \Phi_{n,\alpha}\eta < 1, \\ 0 & \text{for } \xi = \Phi_{n,\alpha}\eta \geqslant 1, \end{cases}$$

$$f'_\alpha = \begin{cases} f''_\alpha(0)\eta & \text{for } \xi = \Phi_{n,\alpha}\eta < \xi_c, \\ \eta^\alpha & \text{for } \xi = \Phi_{n,\alpha}\eta \geqslant \xi_c \end{cases}$$

with $\xi_c = [f''_\alpha(0)]^{1/(\alpha-1)}/\Phi_{n,\alpha}$. When $\xi_c > 1$ (a condition that was found to be satisfied for a large range of values of α and n) the integrals assume the form:

$$\int_0^1 f''_\alpha(0)\eta(1 - \Phi_{n,\alpha}\eta)\,\mathrm{d}\eta = \frac{f''_\alpha(0)}{[\Phi_{n,\alpha}]^2}\int_0^1 \xi(1-\xi)\,\mathrm{d}\xi = \frac{f''_\alpha(0)}{6[\Phi_{n,\alpha}]^2}$$

then:

$$\frac{\Phi_{n,\alpha}}{\Phi_{0,\alpha}} \simeq \zeta\left(\frac{\Phi_{0,\alpha}}{\Phi_{n,\alpha}}\right)^2 \quad\Rightarrow\quad \frac{\Phi_{n,\alpha}}{\Phi_{0,\alpha}} \simeq \zeta^{1/3}. \tag{15}$$

The actual form of the interpolating line is $\zeta^{0.41}$ but the above "order of magnitude" analysis explains the functional dependence.

It is of a certain interest to consider separately the characteristics of the three cases of main practical interest above mentioned, namely the uniform wall temperature ($n = 0$), the uniform wall heat flux ($n = 1 - m(\alpha)$) and the "adiabatic" wall ($n = -m(\alpha)$).

The isothermal wall ($n = 0$). Fig. 6(a) reports the solutions $\Theta^{(0,\alpha)}$ for four values of α for $Pr = 1$. It is evident a non-monotonic behaviour when α changes from $-1/2$ to $1/2$. The slope of the curves at $\eta = 0$ (i.e. $\Phi_{0,\alpha}(Pr = 1) = -\Theta_\eta^{(n,\alpha)}(0)$)

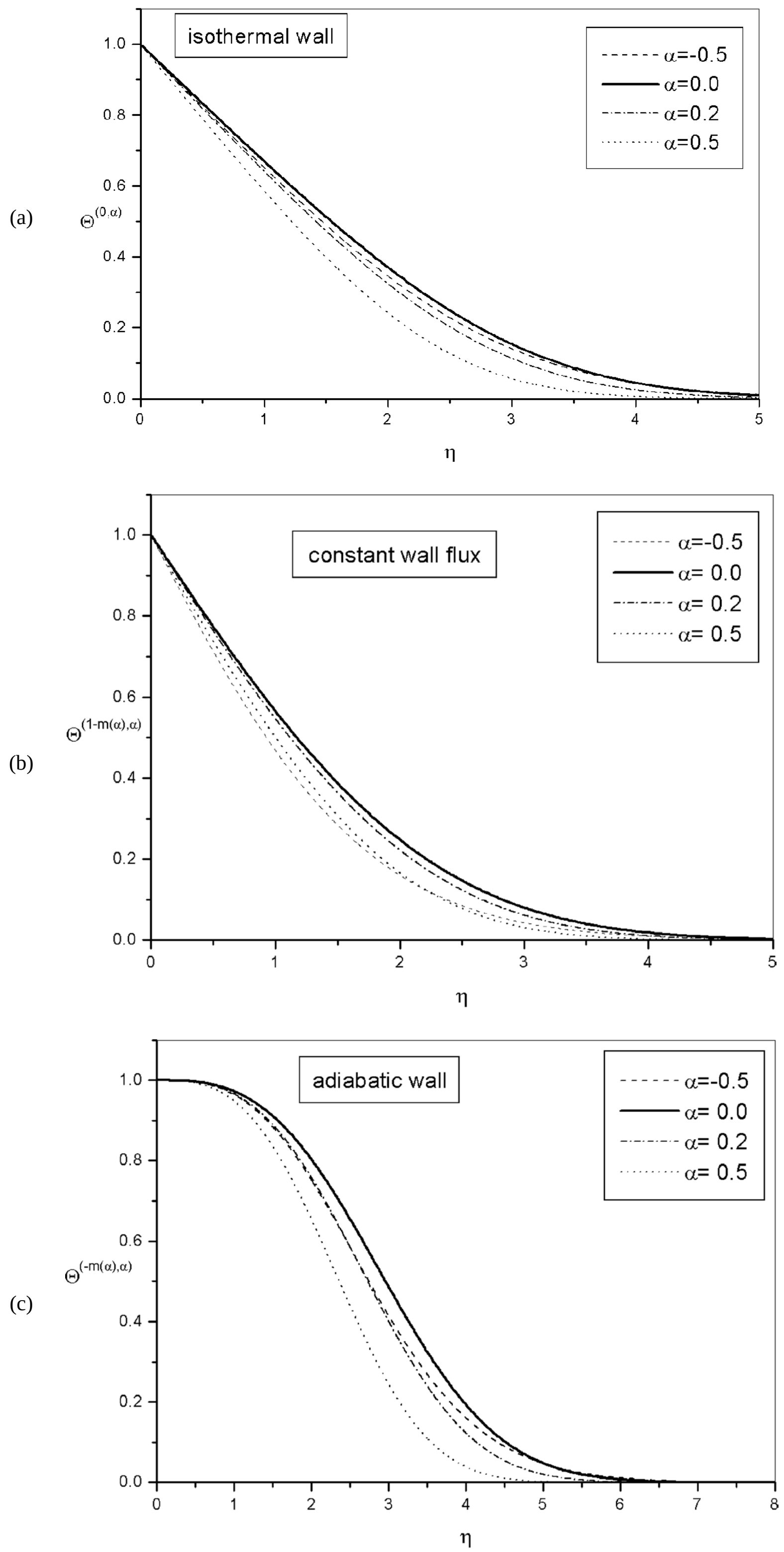

Fig. 6. Non-dimensional temperature profile for some values of α and for: (a) constant wall temperature; (b) constant wall heat flux; (c) adiabatic wall.

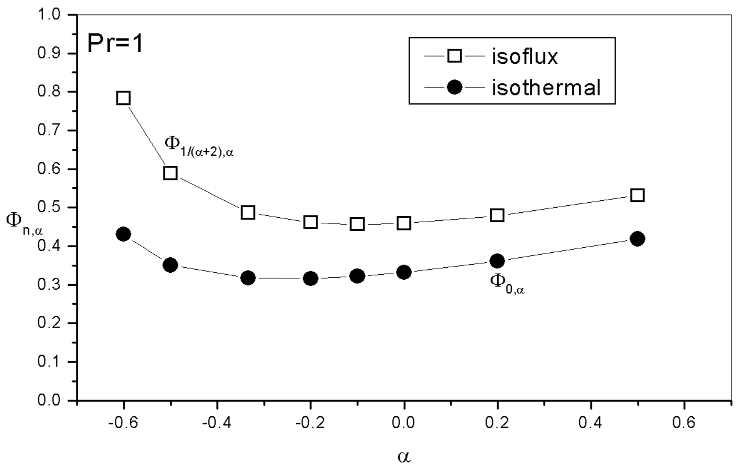

Fig. 7. Non-dimensional temperature gradient at $\eta = 0$ for constant wall temperature and constant wall heat flux.

was then evaluated for different values of α and the results are shown in Fig. 7: a minimum value of $\Phi_{0,\alpha}(Pr = 1) \approx 0.3145$ is found for $\alpha \approx -0.25673$. It is also worth noticing that the integral in Eq. (14) is the non-dimensional thermal (enthalpy) thickness Δ_2 (see [18]), then we may write (for $n \neq -m(\alpha)$):

$$\Delta_2^{n,\alpha} = \frac{\Phi_{n,\alpha}(Pr)}{(m(\alpha)+n)} \tag{16}$$

and for $n = 0$:

$$\Delta_2^{0,\alpha} = \left(\frac{\alpha+2}{\alpha+1}\right)\Phi_{0,\alpha}(Pr) \simeq \left(\frac{\alpha+2}{\alpha+1}\right)C_{0,\alpha}Pr^{1/3}$$

and the value of the thermal thickness for $Pr = 1$ is shown in Fig. 8 for different values of the parameter α. A minimum value of $\Delta_2^{0,\alpha} \approx 0.6565 Pr^{1/3}$ is reached for $\alpha \approx 0.1234$. To notice that the values of $\Delta_2^{n,\alpha}$ were also calculated by a numerical integration of $\int_0^\infty f'_\alpha \Theta^{(n,\alpha)}\,\mathrm{d}\eta$ and found to agree with those calculated from (16) with accuracy better than 0.5%.

The constant flux wall ($n = 1/(\alpha+2)$). The constant flux wall is characterised by a temperature distribution given by the law:

$$T(x,0) - T_\infty = Ax^{1/(\alpha+2)}$$

and by non-dimensional temperature profiles as those reported in Fig. 6(b) for four values of α and for $Pr = 1$. Also in this case the behaviour is non-monotonic when α changes from $-1/2$ to $1/2$ and the non-dimensional temperature gradient at the wall surface ($\Phi_{1/(\alpha+2),\alpha}$ $(Pr = 1)$) was evaluated for different values of α and compared to the results obtained for the isothermal wall in Fig. 7. The dependence on α is similar but the minimum value of $\Phi_{1/(\alpha+2),\alpha}$ $(Pr = 1) \approx 0.4563$ is now reached for $\alpha \approx -0.0944$. The thermal (enthalpy) thickness Δ_2 is now equal to $\Phi_{n,\alpha}(Pr)$ (see Eq. (16)) and it is compared (for $Pr = 1$) to the isothermal case in Fig. 8. The thermal thickness for the constant temperature case is always larger, and the ratio

$$\frac{\Delta_2^{0,\alpha}}{\Delta_2^{1/(\alpha+2),\alpha}} = \left(\frac{\alpha+2}{\alpha+1}\right)\frac{\Phi_{0,\alpha}(Pr)}{\Phi_{1/(\alpha+2),\alpha}(Pr)} \tag{17}$$

is shown in Fig. 9. Applying the approximate result of Eq. (15) to Eq. (17) yields: $\Delta_2^{0,\alpha}/\Delta_2^{1/(\alpha+2),\alpha} \approx m(\alpha)^{-2/3}$, reported also in Fig. 9, where a best fit of the available data, suggesting an exponent equal to -0.528 instead of $-2/3$, is also shown.

The adiabatic wall ($n = -(\alpha+1)/(\alpha+2)$). The limiting case $n = -m(\alpha)$ represents the so called "adiabatic wall" condition, and for $\alpha = -1/2$ it was accurately analysed by Magyari et al. [14]. The general solution is $\Theta^{(-m(\alpha),\alpha)}$, and some profiles are reported in Fig. 6(c), in this case the non-dimensional temperature gradient at the wall surface is always nil. The wall temperature profiles for the adiabatic wall are then given by $T(x,0) = Ax^{-m(\alpha)} + T_\infty$. Apparently, such solutions do not seem meaningful, from a physical point of view, for the impermeable semi-infinite slab. In fact, consider the enthalpy flux through any plane defined by $x = const.$, namely:

$$\dot{H} = \rho c \int_0^\infty \tilde{u}\big[T(x,\eta) - T_\infty\big]\,\mathrm{d}\tilde{y} = \rho c \nu P(x) x^{m(\alpha)} \int_0^\infty f'_\alpha \Theta^{(n,\alpha)}(\eta)\,\mathrm{d}\eta$$

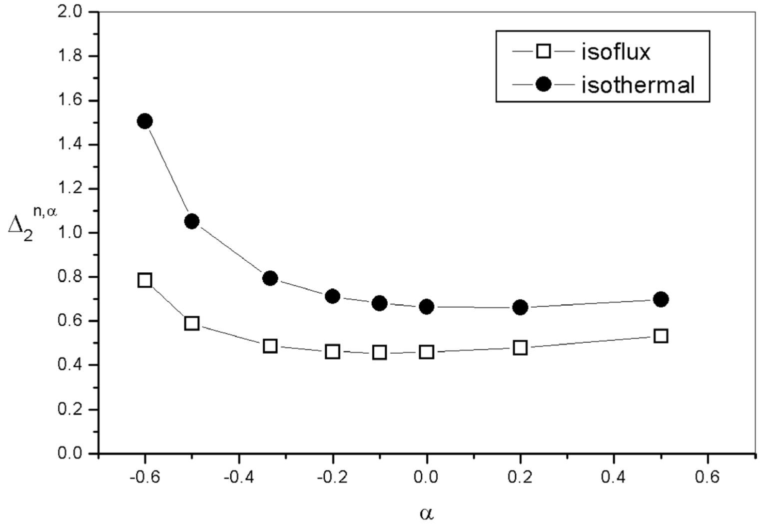

Fig. 8. Value of the thermal thickness $\Delta_2^{n,\alpha}$ vs α for $Pr = 1$ for the constant wall temperature ($n = 0$) and constant wall heat flux ($n = 1 - m(\alpha)$).

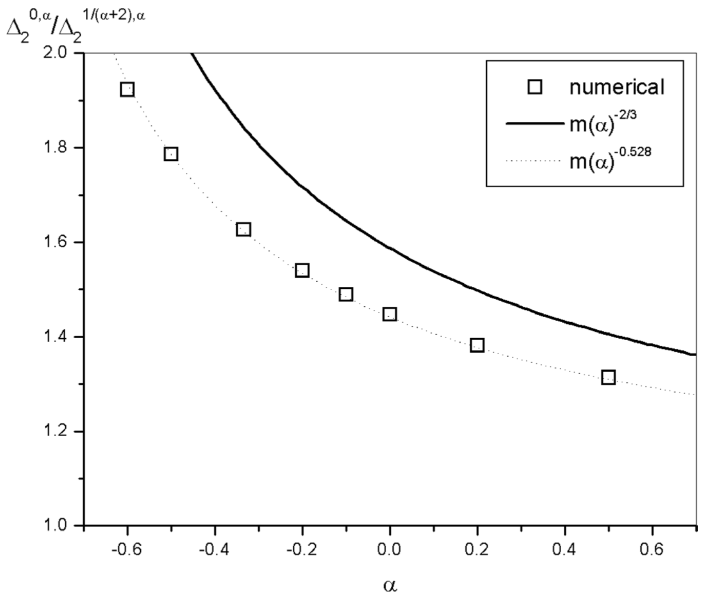

Fig. 9. Ratio of constant temperature thermal thickness and constant flux thermal thickness vs α.

then, neglecting heat conduction in the x direction, the energy balance over an element of the boundary layer gives:

$$\frac{\mathrm{d}\dot{H}}{\mathrm{d}x} = q_w = 0 \tag{18}$$

where the last equality holds for an adiabatic wall (the same result can be obtained by integrating directly the energy equation accounting for all the boundary conditions). It is then clear that any solution of the form $T = P(x)\Theta(\eta) + T_\infty$ can satisfy (18) only if $P = Ax^{-m(\alpha)}$. But, for the semi-infinite slab with no heat input, the initial condition is evidently: $\dot{H}(0) = 0$, thus $P(x)x^{m(\alpha)} = 0$, yielding the trivial solution: $T_w = T_\infty$. However, consider the case with a point-like heat source positioned at

$x = 0$, then the initial condition for Eq. (18) becomes: $\dot{H}(0) = Q$, where Q is the strength of the energy source at $x = 0$. This yields:

$$\rho c \nu P(x) x^{m(\alpha)} \int_0^\infty f'_\alpha \Theta^{(-m(\alpha),\alpha)}(\eta)\,\mathrm{d}\eta = Q$$

i.e.

$$P(x) = \frac{Q}{\rho c \nu \Delta_2^{(-m(\alpha),\alpha)}} x^{-m(\alpha)}$$

that is the non-trivial solutions for the adiabatic case.

4. Validity of the similarity solutions

The momentum and energy equations (3), (4) were obtained under the assumptions $\partial^2 u/\partial x^2 \ll \partial^2 u/\partial y^2$ and $\partial^2 T/\partial x^2 \ll \partial^2 T/\partial y^2$. Considering the full form of the equations:

$$u\frac{\partial u}{\partial x} + v\frac{\partial u}{\partial y} - \frac{\partial^2 u}{\partial y^2} = \frac{\partial^2 u}{\partial x^2},$$
$$Pr\left(u\frac{\partial T}{\partial x} + v\frac{\partial T}{\partial y}\right) - \frac{\partial^2 T}{\partial y^2} = \frac{\partial^2 T}{\partial x^2}$$

by the similarity transformation (5) they become:

$$\left[f''' + mff'' - f'f'(2m-1)\right] = \frac{(1-m)}{x^{2m}}\left[f'''\eta^2(m-1) + f''\eta[5m-4] + f'2(2m-1)\right], \tag{19}$$

$$Pr\,xf'T_x - mPr\,fT_\eta - T_{\eta\eta} = \frac{1}{x^{2m}}\left[T_{\eta\eta}\eta^2(m-1)^2 + T_\eta\eta(m-2)(m-1) + x^2T_{xx}\right] \tag{20}$$

where again $m = (\alpha+1)/(\alpha+2)$. Now it is worth to consider the conditions under which such equations admit similarity solutions.

4.1. *The case $\alpha > -1$*

Let first suppose that $\alpha > -1$, then $m(\alpha) > 0$. When x becomes large, the RHS of Eq. (19) becomes negligible and Eq. (6) is recovered. For the energy equation, choosing again:

$$T = P(x)\Theta(x,\eta) + T_\infty,$$
$$\Theta(0) = 1; \qquad \Theta(\infty) = 0$$

we obtain:

$$Pr\,xf'\frac{P_x}{P}\Theta + Pr\,xf'\Theta_x - mPr\,f\Theta_\eta - \Theta_{\eta\eta} = x^{-2m}\left[\Theta_{\eta\eta}\eta^2(m-1)^2 + \Theta_\eta\eta(m-2)(m-1)\right] + x^{-2m}\left(x^2\frac{P_{xx}}{P}\Theta + 2x^2\frac{P_x}{P}\Theta_x + x^2\Theta_{xx}\right)$$

and, on searching for a solution Θ that is explicitly independent of x, the equation becomes:

$$Pr\,f'x\frac{P_x}{P}\Theta - mPr\,f\Theta_\eta - \Theta_{\eta\eta} = x^{-2m}\left[\Theta_{\eta\eta}\eta^2(m-1)^2 + \Theta_\eta\eta(m-2)(m-1)\right] + x^{-2m}\left(x^2\frac{P_{xx}}{P}\Theta\right)$$

and to have such a solution when $x \to \infty$ the necessary and sufficient condition is $xP_x/P = n$, as in fact:

$$x^2\frac{P_{xx}}{P} = n(n-1); \qquad \lim_{x\to\infty} x^{-2m}\left(x^2\frac{P_{xx}}{P}\right) = 0$$

and Eq. (9) is recovered. This shows that Eqs. (6) and (9) and the relative similarity solutions, discussed in the previous section, hold for large values of x. To better capture the meaning of “large values of x”, consider the classical case $\alpha = 0$, then:

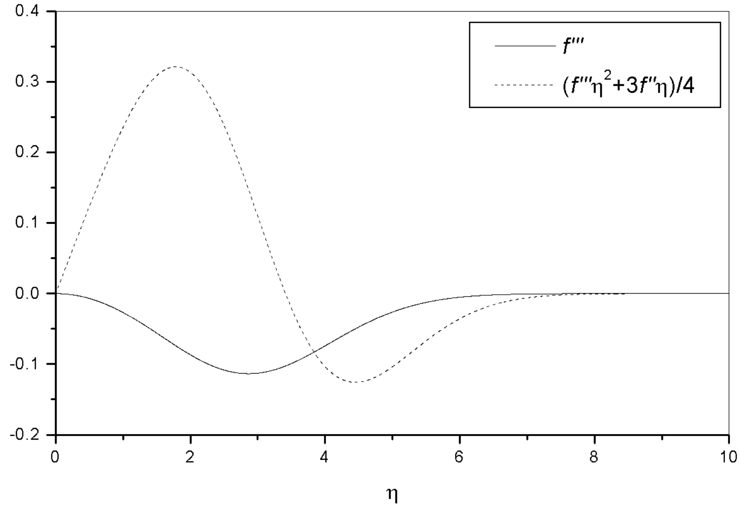

Fig. 10. Magnitude of f''' and $\frac{1}{4}[f'''\eta^2 + 3f''\eta]$ (proportional to the retained and neglected term in the Laplacian) for $x = 1$.

$$f''' + \frac{1}{2}ff'' = -\frac{1}{4x}[f'''\eta^2 + 3f''\eta],$$
$$\Theta_{\eta\eta} + \frac{1}{2}Pr\, f\Theta_\eta - Pr\, f'n\Theta = -\frac{1}{4x}\left[\Theta_{\eta\eta}\eta^2 + 3\Theta_\eta\eta + 4n(n-1)\Theta\right]$$

with B.C.:

$$f(0) = 0; \qquad f'(0) = 0; \qquad f'(\infty) = \beta = \frac{U_\infty L}{\nu},$$
$$\Theta(0) = 1; \qquad \Theta(\infty) = 0.$$

Choosing $\beta = 1$, the maximum value of x for which the problem still retains a practical interest is: $x_{\max} = Re_c$ where Re_c is the critical Reynolds number for transition to turbulence ($Re_c = 5 \cdot 10^5$ for the present case). Fig. 10 shows a comparison between f''' and $\frac{1}{4}[f'''\eta^2 + 3f''\eta]$ (proportional to the retained and neglected term in the Laplacian) showing that already for $x/x_{\max} > 10^{-3}$ the peek value of the neglected term in the Laplacian is less than 0.6% of the retained one. An identical result can obviously be obtained for the energy equation in the case $Pr = 1$, and $n = 0$.

Consider now the case $x \to 0$. In such a case the asymptotic form of the momentum equation becomes:

$$f'''\eta^2(m-1) + f''\eta[5m-4] + f'2(2m-1) = 0$$

i.e. an Euler equation whose solutions are given by:

$$f' = B\eta^{-2} + C\eta^\alpha$$

(having excluded the case $\alpha = -2$ that gives $m(\alpha) = \infty$) but it is clear that the B.C.:

$$f(0) = 0; \qquad f'(0) = 0; \qquad f'(\infty) = \beta\eta^\alpha$$

cannot all be satisfied. This means that similarity solutions for $x \to 0$ do not exist, implying a similar result also for the energy equation.

4.2. *The case* $\alpha < -1$

In this case the function $m(\alpha)$ is negative and, for large values of x, Eq. (19) becomes:

$$f'''\eta^2(m-1) + f''\eta[5m-4] + f'2(2m-1) = 0 \tag{21}$$

and, as shown above, this equation cannot satisfy the boundary conditions, for any negative value of the function $m(\alpha)$. For $x \to 0$ the momentum and energy equations become:

$$f''' + mff'' - f'f'(2m-1) = 0,$$
$$\Theta^{(n,m)}_{\eta\eta} + m\,Pr\, f_m\Theta^{(n,m)}_\eta - Pr\, f'_m n\Theta^{(n,m)} = 0$$

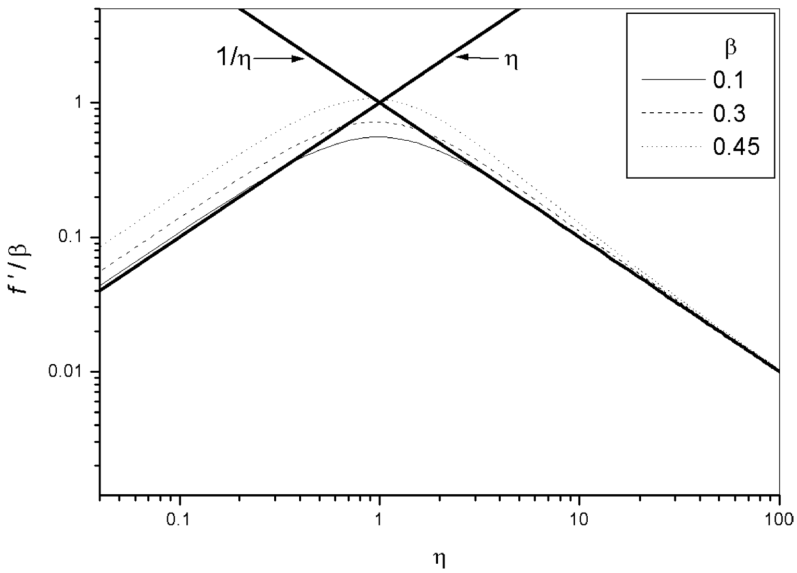

Fig. 11. Numerical solutions of the momentum equation when $\alpha = -1$ for different values of β.

but it was already mentioned that this momentum equation admits similarity solutions satisfying the given boundary condition only for $1 > m(\alpha) > 1/4$, thus excluding any solution also for small values of x.

4.3. The case $\alpha = -1$

In this case $m(\alpha) = 0$ and the momentum equation becomes:

$$f'''(1+\eta^2) + 4f''\eta + f'f' + 2f' = 0,$$
$$f(0) = 0; \qquad f'(0) = 0; \qquad f'(y=\infty) = \beta\eta^{-1}$$

but now for this particular value of α the value $\beta = \gamma/\nu$ is independent of the choice of the characteristic length. This makes a difference, as now the solutions found for different values of β do not follow the scaling law (8). Fig. 11 shows the numerical solutions for different values of β.

The similarity solution of the energy equation should satisfy the equation:

$$\Theta_{\eta\eta}(1+\eta^2) + 2\Theta_\eta\eta + x^2\frac{P_{xx}}{P}\Theta - Pr\, f'x\frac{P_x}{P}\Theta = 0$$

with the conditions:

$$x\frac{P_x}{P} = n; \qquad x^2\frac{P_{xx}}{P} = q$$

thus obtaining $q = n(n-1)$ and:

$$\Theta_{\eta\eta}(1+\eta^2) + 2\Theta_\eta\eta + (n-1-Pr\, f')n\Theta = 0.$$

The case with a uniform wall temperature ($n = 0$) shows a particular behaviour. The problem reduces to:

$$\Theta_{\eta\eta}(1+\eta^2) + 2\Theta_\eta\eta = 0,$$
$$\Theta(0) = 1; \qquad \Theta(\infty) = 0$$

that admits an analytical solution that is independent of the actual velocity field:

$$\Theta = -\frac{2}{\pi}\arctan(\eta) + 1,$$
$$\Theta_\eta = -\frac{2}{\pi(1+\eta^2)},$$
$$\Phi_{n,\alpha}(Pr) = -\Theta_\eta^{(n,\alpha)}(0) = \frac{2}{\pi} = 0.63662.$$

5. Conclusions

The problem of steady forced convection thermal boundary-layer driven by a power-law shear has been considered. The search for similarity solutions of the momentum and energy equations introduces three parameters: "α" the exponent of the decaying exterior velocity profile, "n" the exponent of the prescribed thermal condition on the wall necessary to obtain similarity solutions and the Prandtl number. The dependence of the non-dimensional wall temperature gradient (proportional to the local Nusselt number) on the Prandtl number was found to follow the 1/3-law (for a large range of Prandtl number values) for any thermal boundary condition that assures the existence of a similarity solution. A common dependence of the same parameter on (α, n) was also found under the form of a power-law.

A critical analysis of the assumptions usually accepted to derive similarity solutions in boundary layer flow was performed. The range of validity of the similarity solution was then quantified for the full range of values of the parameter α. For $\alpha > -1$, the classical momentum and energy ordinary differential equations hold and similarity solutions were seen to be an acceptable description of the flow for large values of the coordinate x, whereas for $x \to 0$ no similarity solutions exist. For $\alpha < -1$ the differential equations describing the flow are modified, and no similarity solutions are shown to exist for any value of x. For $\alpha = -1$ a possible solution is found for an isothermal wall.

References

[1] L. Prandtl, Uber Flussigkeitsbewegung bei sehr kleiner Reibung, in: Proc. 3rd Int. Math. Congr., Heidelberg, 1904, pp. 484–491. Translated in English as: Motion of fluids with very little viscosity, NACA TM 452-1928.
[2] H. Blasius, Grenzschichten in Flussigkeiten mit kleiner Reibung, Z. Math. Phys. 56 (1908) 1–37. Translated in English as: The boundary layer in fluids with little friction, NACA TM 1256, 1956.
[3] K. Pohlhausen, Der Warmeaustausch zwichen festen Korpen und Flussigkeiten mit kleiner Reibung und kleiner Warmeleitung, Z. Angew. Math. Mech. 1 (1921) 115–121.
[4] W.H.H. Banks, Similarity solutions of the boundary layer equations for a stretching wall, J. Mech. Theor. Appl. 2 (1983) 375–392.
[5] L. Crane, Flow past a stretching plate, Z. Angew. Math. Phys. 21 (1970) 645–647.
[6] E. Magyari, B. Keller, Exact solutions for self-similar boundary-layer flows induced by permeable stretching walls, Eur. J. Mech. B Fluids 19 (2000) 109–122.
[7] E. Magyari, I. Pop, B. Keller, New analytical solutions of a well-known boundary value problem in fluid mechanics, Fluid Dynamics Res. 33 (2003) 313–317.
[8] H.K. Kuiken, On boundary layers in fluid mechanics that decay algebraically along stretches of walls that are not infinitesimally small, IMA J. Appl. Math. 27 (1981) 387–405.
[9] D.B. Ingham, I. Pop, Transport Phenomena in Porous Media, Pergamon, Oxford, 2002.
[10] D.A. Nield, A. Bejan, Convection in Porous Media, Springer, New York, 1999.
[11] P.D. Weidman, D.G. Kubitschek, S.N. Brown, Boundary layer similarity flow driven by power-law shear, Acta Mech. 120 (1997) 199–215.
[12] E. Magyari, B. Keller, I. Pop, Boundary layer similarity flows driven by a power-law shear over a permeable plane surface, Acta Mech. 163 (2003) 139–146.
[13] S.-J. Liao, I. Pop, Explicit analytical solution for similarity boundary layer equations, Int. J. Heat Mass Transfer 47 (2004) 75–85.
[14] I. Magyari, E. Kelle, B. Pop, Heat transfer characteristics of a boundary-layer flow driven by a power-law shear over a semi-infinite plate, Int. J. Heat Mass Transfer 47 (2004) 31–34.
[15] A. Bejan, Convection Heat Transfer, Wiley, New York, 1995.
[16] E.M. Sparrow, S.H. Lin, Boundary layer with prescribed heat flux-application to simultaneous convection and radiation, Int. J. Heat Mass Transfer 8 (1965) 437–448.
[17] G. Polidori, M. Rebay, J. Padet, Retour sur les rśultats de la théorie de la convection forcée laminaire étabilie en écoulement de couche limite externe 2D, Int. J. Therm. Sci. 38 (1999) 398–409.
[18] W.M. Kays, M.E. Crawford, Convective Heat and Mass Transfer, third ed., McGraw-Hill, New York, 1993, p. 71.